## Title

Hydrogen-bonding-induced efficient dispersive solid phase extraction of bisphenols and their derivatives in environmental waters using surface amino-functionalized MIL-101(Fe)



## Authors

Gao, Man
Liu, Wei
Wang, Xuran
et al.

## Publication Date

2019-03-01

## DOI

10.1016/j.microc.2018.12.013

Peer reviewed

Microchemical Journal 145 (2019) 1151–1161

Contents lists available at ScienceDirect

Microchemical Journal

journal homepage: www.elsevier.com/locate/microc

# Hydrogen-bonding-induced efficient dispersive solid phase extraction of bisphenols and their derivatives in environmental waters using surface amino-functionalized MIL-101(Fe)

Man Gao[a,1], Wei Liu[a,1], Xuran Wang[b], Yanyan Li[a], Peipei Zhou[a], Liwan Shi[a], Buxing Ye[a], Randy A. Dahlgren[a], Xuedong Wang[a,c,*]

[a] Zhejiang Provincial Key Laboratory of Watershed Science and Health, College of Public Health and Management, Wenzhou Medical University, Wenzhou 325035, China
[b] School of Materials Science & Engineering, University of Science & Technology Beijing, Beijing 100083, China
[c] National and Local Joint Engineering Laboratory of Municipal Sewage Resource Utilization Technology, School of Environmental Science and Engineering, Suzhou University of Science and Technology, Suzhou 215009, China

ARTICLE INFO

*Keywords:*
Hydrogen-bonding interaction
$NH_2$-MIL-101(Fe)
Dispersive solid-phase extraction
Bisphenols and derivatives
Environmental waters

ABSTRACT

Herein, we investigated in detail the relationship between surface properties and extraction performance of virgin and amino-functionalized MIL-101s(Fe) for the extraction of 10 bisphenols (BPs) and their derivatives. These BPs were used as model contaminants due to their different hydroxyl groups and contrasting polarities. The differential sorption efficiencies for relatively polar BPs (BPF, BPE, BPA, BPB, BPZ, BPAP and BPP) lies in the formation of hydrogen-bonding between −OH of target analytes and $-NH_2$ of two MIL-101s(Fe). However, the surface properties of MIL-101(Fe) and $NH_2$-MIL-101s(Fe), such as $S_{BET}$ and pore structure, determined the extraction recoveries for BPs derivatives (BADGE, BADGE·$2H_2O$ and BFDGE·$2H_2O$) due to lack of −OH in their molecular structures. $NH_2$-MIL-101s(Fe) nanosorbent was successfully applied to the preconcentration/extraction of trace BPs and their derivatives by dispersive solid-phase extraction (DSPE) method. Following optimization of the main factors, recoveries for BPs ranged from 90.8 to 117.8% and their LODs were 0.016–0.131 μg $L^{-1}$ in environmental waters. Experimental precisions based on relative standard deviations were 0.9–4.9% for intra-day and 1.3–7.6% for inter-day analyses, respectively. These findings provide important information on how to design and modify nanosorbents for highly efficient extraction of pollutants having contrasting polarities. Moreover, the newly developed $NH_2$-MIL-101s(Fe)-based DSPE method has a good application prospect in pretreatment of trace pollutants in real-world waters.

## 1. Introduction

For the past several decades, there has been increasing awareness and concern for health threats caused by endocrine-disrupting chemicals (EDCs) that interfere with hormone biosynthesis and metabolism, or alter activity from normal homeostatic control or reproduction [1]. Among the numerous EDCs, bisphenol A (BPA) has received particular attention because of its widespread occurrence and toxicity. Furthermore, a series of structural analogues and derivatives of BPA has emerged as potential EDCs, including bisphenol B (BPB), bisphenol E (BPE), bisphenol F (BPF), bisphenol diglycidyl ethers (BDGEs) and BDGEs derivatives. These compounds possess similarly acute toxicity, genotoxicity, and estrogenic activity with some exhibiting higher toxicity than BPA [2–4]. The occurrence and distribution of BPA in various environmental matrices and human samples, such as air, surface water, waste water, sewage sludge, aquatic sediments, house dust, foodstuffs, urine, blood, and human breast milk, have been widely documented in the scientific literature [5–7]. Additionally, bisphenol analogues and derivatives in personal care products (PCPs), foodstuffs and a variety of environmental matrices, including indoor dust, sediments, fresh and sea waters, sewage effluent and sludge, have been extensively documented [8]. For example, BPF was the most abundant bisphenol analogue in surface waters from sites in Japan, Korea, and China, contributing > 70% of total BP concentrations [9]. This may reflect high usage of BPF as a BPA replacement in southeastern Asia. Similarly, BPF was found as the second most abundant BP analogue in a

* Corresponding author at: Zhejiang Provincial Key Laboratory of Watershed Science and Health, College of Public Health and Management, Wenzhou Medical University, Wenzhou 325035, China.
*E-mail address:* zjuwxd@163.com (X. Wang).
[1] Co-first author: Man Gao and Wei Liu are equal to the first author.

https://doi.org/10.1016/j.microc.2018.12.013
Received 8 September 2018; Received in revised form 11 November 2018; Accepted 10 December 2018
Available online 11 December 2018
0026-265X/ 

USA food survey, including beverages, dairy products, fats and oils, fish and seafood, meat, cereals, fruits, and vegetables [10]. Further, BPA, BPS, and BPF were the major contributors accounting for > 98% of total BPs in indoor dust samples from the USA and several Asian countries [11].

Ultra-low concentrations coupled with the complexity of environmental samples pose major challenges for BP analysis in real-world samples. Dispersive solid-phase extraction (DSPE) is an expanded SPE procedure that maintains the advantages of SPE and also benefits from simple operation, short extraction time and higher recovery efficiency. In DSPE, the sorbent plays a crucial role in determining extraction efficiency.

Metal-organic frameworks (MOFs) are a class of hybrid inorganic-organic micro-porous crystalline material formed through self-assembly of metal ions or clusters and organic ligands via coordination bonds [12]. The interest in MOF-type materials is growing due to several strategic characteristics, including large porosity and surface area, easy tunability of pore size and shape from microporous to mesoporous scale, and adjustable internal surface properties. Furthermore, the central metals, coordinatively unsaturated sites (CUS or open metal sites), functionalized linkers, and loaded active species, have been successfully employed to provide additional interactions between adsorbates and MOF-type materials. These properties make MOFs superior to other porous adsorbents for efficient adsorption of several hazardous compounds [13]. Owing to these properties, MOF-type materials have been used in a wide variety of applications, such as gas storage [14], adsorption [15,16], drug delivery [17,18], polymerization [19], magnetism [20], catalysis [21], and luminescence [22]. MIL-101(Fe) (MIL, Material Institute Lavoisier) is an acid-stable, hydrophilic MOF [23] having a zeotype crystal structure with high resistance to air, water and common solvents [24,25], which are key properties for application as an adsorbent in pretreatment of environmental samples. Hence, MIL-101(Fe) was selected as a model adsorbent for extraction of trace BPs from environmental samples in this study.

MOF-type materials have been widely investigated in the field of analytical chemistry. Several examples for MIL-101 include use in the enrichment step of organophosphorus pesticides in biological samples [24], imatinib mesylate in plasma [26] polycyclic aromatic hydrocarbons (PAHs) in environmental water samples [27], and phthalate esters in water samples and human plasma [28]. These studies demonstrate the efficacy of MOFs as an effective pretreatment for organic compounds from a variety of matrices. For the same type of analytes, some pristine (i.e., non-modified) MOFs provide higher adsorption efficiency for weakly polar chemicals than highly polar compounds. For example, MOF-5 showed increased sorption of PAHs with increasing log $K_{ow}$ values (*n*-octanol/water partition coefficients) [29]. Because some pristine MOFs have poor sorption efficiency for analytical pretreatments, several studies have modified MOF composites to enhance extraction performance. However, the preparation of hybrid MOFs is often cumbersome and it is difficult to achieve the desired result. Moreover, the selection of elution solvent is more critical when using composites since certain solvents can destroy the structure of composites complicating their use [30].

Among the various host-guest interactions between adsorbates and adsorbents, acid-base, π-complexation, H-bonding and coordination with open metal sites play important roles in regulating adsorption affinity [13]. Currently, hydrogen bonding has been regarded as an important mechanism to explain sorption of polar organics on functionalized MOFs [31]. Herein, we investigated the extraction performance of 10 BPs (hydroxyl-containing and non-hydroxyl-containing) on MIL-101s (virgin and functionalized with amino groups) to understand the effect of hydrogen bonding on adsorption of bisphenols and their derivatives from water. The properties of the DSPE adsorbents were characterized, and several operational parameters were investigated to optimize extraction efficiency. This $NH_2$-MIL-101(Fe)-based DSPE method exhibits good prospects for extraction of BPs from environmental samples.

## 2. Experimental section

### 2.1. Chemicals and materials

Analytical grade ferric chloride hexahydrate ($FeCl_3{\cdot}6H_2O$), 2-aminoterephthalic acid ($NH_2$-BDC), terephthalic acid ($H_2BDC$) and phosphoric acid were purchased from Sinopharm Chemical Reagent Co. (Shanghai, China). *N*, *N*-dimethylformamide (DMF, AR) was acquired from Aladdin Chemistry (Shanghai, China). Standards of bisphenol F (BPF, ≥99.9%), bisphenol A (BPA, ≥98.5%), bisphenol AP (BPAP, ≥99.8%) and bisphenol B (BPB, ≥99.8%) were obtained from Dr. Ehrenstorfer (Augsburg, Germany). Bisphenol E (BPE, 100%), bisphenol Z (BPZ, 100%), bisphenol P (BPP, ≥99.5%) and bisphenol A diglycidyl ether (BADGE, ≥99.1%) were purchased from AccuStandard (New Haven, CT, USA). $BFDGE{\cdot}2H_2O$ (≥95.0%) and $BADGE{\cdot}2H_2O$ (≥97.0%) were obtained from Sigma-Aldrich (St. Louis, MO, USA). Table 1 lists chemical structures and selected physicochemical properties for these compounds. All chemicals were used as received without further purification. HPLC-grade methanol, ethanol, acetone, and acetonitrile were purchased from Merck (Darmstadt, Germany). Ultrapure water (> 18.2 MΩ-cm, Millipore, Billerica, MA, USA) was used for all experiments. The 0.22 μm nylon (NL) and 0.45 μm polyether sulfone (PES) membrane filters were purchased from Anpel Scientific Instrument Co. (Shanghai, China).

### 2.2. Instrumentation

A Chromaster Infinity HPLC system (Hitachi, Japan) equipped with a Zorbax Eclipse SB-C18 column (150 mm × 4.6 mm, 5 μm) was used for BP analysis. MOF separation was achieved using a high speed centrifuge (HC-3518, Anhui USTC Zonkia Scientific Instruments. Hefei, China). A KQ-300VDE ultrasonic cleaner was used in the extraction step at a frequency and output power of 45 kHz and 300 W, respectively (Kunshan Ultrasonic Instruments. Kunshan, China). Solution pH was measured with a PB-10 pH meter (Sartorius, Göttingen, Germany). Samples were mixed with a XH-D vortex mixer (Shanghai Zhengqiao Scientific Instruments. Shanghai, China) and phase separation was achieved using a model TDL-50C centrifuge (Anting Instrument, Shanghai, China).

### 2.3. Synthesis of Fe-based MIL-101s

$NH_2$-MIL-101(Fe) was synthesized by a simple solvothermal method with minor modification [32]. Briefly, $FeCl_3{\cdot}6H_2O$ (19.75 mmol) and $NH_2$-BDC (10.0 mmol) were dissolved in 60 mL of DMF and magnetically stirred for 10 min. The mixture was then transferred to a 100 mL Teflon-lined stainless steel autoclave and heated at 110 °C for 24 h followed by cooling to room temperature. A brown solid product was obtained by centrifuging, sequential rinsed with DMF, deionized water and ethanol, and then dried in a vacuum oven at 60 °C for 6 h. MIL-101(Fe) was synthesized using the same method with $H_2BDC$ replacing $NH_2$-BDC as a substrate.

### 2.4. Characterization of Fe-based MIL-101s

X-ray diffraction (XRD) patterns in the range of 5 to 30° (2θ) were obtained using a Bruker D8 Advance X-ray diffractometer with Cu Kα radiation (λ = 1.5418 Å) operated at 40 kV and 40 mA (Bruker, Billerica, MA, USA). Scanning electron microscopy (SEM) was conducted on a Sigma 300 VP scanning electron microscope (Carl Zeiss, Jena, Germany). Nitrogen adsorption and desorption isotherms at 77 K were measured with an ASAP 2020 M (Micromeritics Instruments, Norcross, GA, USA). Fourier transform infrared (FT-IR) spectra were recorded on a Nicolet IS50 FTIR Spectrometer (ThermoFisher Scientific, Waltham, MA, USA) in the range of 400–4000 $cm^{-1}$ using KBr pellets. Zeta potentials were obtained using a Zetasizer Nano-ZS (Malvern

**Table 1**
Chemical structure, ionization constants, *n*-octanol/water partition coefficients and number of H-bond acceptors and donors for the target compounds.

| Compound | Structure | p$Ka_1$[a] | p$Ka_2$[a] | Log $K_{ow}$[b] | Number of H-bond acceptor | Number of H-bond donor |
|---|---|---|---|---|---|---|
| Bisphenol F (BPF) | 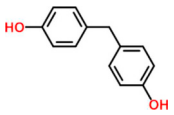 | 9.91 | 10.50 | 2.73 | 2 | 2 |
| Bisphenol E (BPE) | 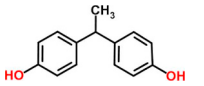 | 10.10 | 10.74 | 3.08 | 2 | 2 |
| Bisphenol A (BPA) | 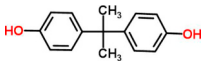 | 10.29 | 10.93 | 3.43 | 2 | 2 |
| Bisphenol B (BPB) | 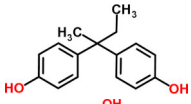 | 10.27 | 10.91 | 3.96 | 2 | 2 |
| Bisphenol AP (BPAP) | 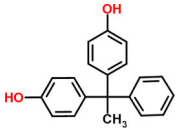 | – | – | 4.57 | 2 | 2 |
| Bisphenol Z (BPZ) | 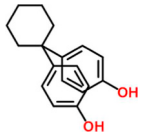 | – | – | 4.53 | 2 | 2 |
| Bisphenol P (BPP) | 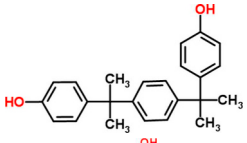 | – | – | 6.12 | 2 | 2 |
| Bisphenol F bis(2,3-dihydroxypropyl) ether (BFDGE·2$H_2O$) | 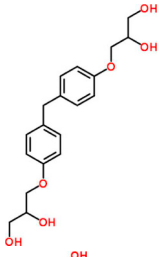 | – | – | 1.17 | 6 | 4 |
| Bisphenol A bis(2,3-dihydroxypropyl) ether (BADGE·2$H_2O$) | 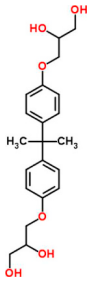 | 14.72 | 15.32 | 1.86 | 6 | 4 |
| Bisphenol A diglycidyl ether (BADGE) | 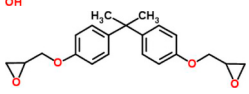 | – | – | 3.95 | 4 | 0 |

[a] Data calculated from http://ilab.acdlabs.com/ilab2 (ACD LABS).
[b] Data predicted using ACD log P searched from http://www.chemspider.com/ (ChemSpider).

Instruments, Malvern, UK). Water contact angles were measured on a contact angle measurement system OCA 20 (DataPhysics, Filderstadt, Germany).

### 2.5. Preparation of standard solutions and real-world water samples

An individual stock solution of BPs (100 mg $L^{-1}$) was prepared by dissolving each BP standard in methanol with subsequent storage at 4 °C in the dark to avoid photochemical degradation. Mixed BP working solutions (10 mg $L^{-1}$) were prepared fresh by dilution of each individual stock solution with methanol. All standard solutions were protected from light and brought to ambient laboratory temperature prior to use.

A river water sample was obtained from the urban portion of the Wenruitang River, Wenzhou, China. Sea water was collected from a coastal area near Yanting Town, Cangnan, China. Tap water was taken

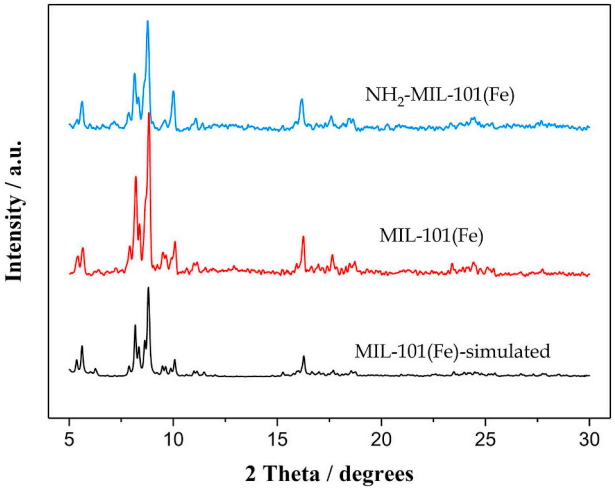


**Fig. 1.** XRD patterns of simulated MIL-101(Fe) (black), as-synthesized MIL-101(Fe) (red), and $NH_2$-MIL-101(Fe) (blue).

directly from our laboratory at Wenzhou Medical University, Wenzhou, China. All water samples were filtered through a 0.45 μm PES membrane filter, and stored in a precleaned, light-preserved glass bottle at 4 °C until use.

### 2.6. DSPE procedures and chromatographic analyses

In a typical DSPE procedure, 5 mL of BP sample solution (20.0 μg $L^{-1}$) was added to a 15 mL screwcap glass conical centrifuge tube to which 10–50 mg of extractant ($NH_2$-MIL-101(Fe)) was added to the solution and ultrasonicated for 1.0–5.0 min. The extractant was separated from the suspension by centrifugation at 5000 rpm for 10 min. After decanting the supernatant, the extractant was eluted using 0.1–0.8 mL desorption solvent and vortexing for 1.0–5.0 min. The mixture was finally centrifuged at 5000 rpm for 3 min, and the resulting supernatant was utilized for chromatographic analysis.

BP concentration was determined by a high performance liquid chromatography equipped with a fluorescence detector (HPLC-FLD). The mobile phase was composed of phosphoric acid in water (pH = 3.0, B) and acetonitrile (C), and the optimized gradient elution program followed: 0–3.0 min, 30% C; 3.1–4.0 min, 30%–40% C; 4.1–17.0 min, 40% C; 17.1–18 min, 40%–30% C and 18–22 min, 30% C. Flow rate was 1.0 mL $min^{-1}$, column temperature was maintained at 30 °C, and the sample loop volume was 10 μL. Fluorescence excitation and emission wavelengths were 233 and 303 nm, respectively.

## 3. Results and discussion

### 3.1. Characterization

XRD was employed to evaluate the crystallinity and phase purity of the as-prepared products (Fig. 1). The diffraction peaks of the as-prepared products were well matched with the standard reference peaks of MIL-101(Fe) indicating successful preparation. Moreover, the dominant diffraction peaks of $NH_2$-MIL-101(Fe) were the same as MIL-101(Fe) indicating a similar crystal structure for the two MOFs [33]. A detailed analysis of the X-ray peak broadening (at ca. 8.8°) of MIL-101(Fe) and $NH_2$-MIL-101(Fe) using the Scherrer equation indicates that the crystallite size are ca. 45.2 nm and ca. 36.6 nm, respectively. SEM images characterizing the morphologies of $NH_2$-MIL-101(Fe) and MIL-101(Fe) are shown in Fig. 2. Both MOFs have a uniform octahedral nanocrystalline structure; however, $NH_2$-MIL-101(Fe) exhibited smaller crystal size than MIL-101(Fe) (Fig. 2C and D) [33,34].

Nitrogen sorption was employed to investigate structural properties of the as-prepared MIL-101s (Fig. S1). The $S_{BET}$ surface area, average pore volume and pore diameter of $NH_2$-MIL-101(Fe) were 2914 $m^2 \cdot g^{-1}$, 1.46 $m^3 \cdot g^{-1}$ and 2.19 nm, respectively, which were slightly lower than those of MIL-101(Fe) (3067 $m^2 \cdot g^{-1}$, 1.79 $m^3 \cdot g^{-1}$ and 2.24 nm). The high specific surface area and large pore size of these two MOFs are advantageous for their potential application in adsorption and extraction of organic compounds [35].

Due to the specific effects of surface functional groups on adsorption and extraction of organic chemicals, FT-IR was used to characterize

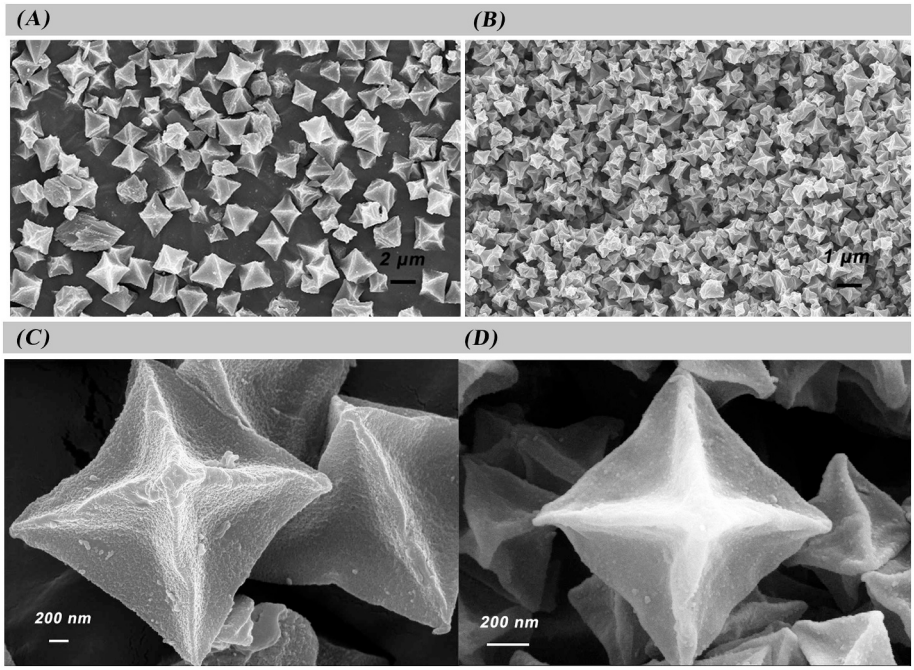


**Fig. 2.** Scanning electron microscopy (SEM) images of MIL-101(Fe) (A, C) and $NH_2$-MIL-101(Fe) (B, D).

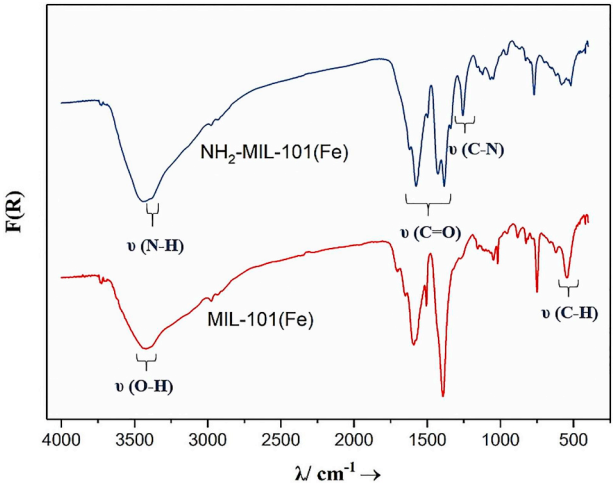


**Fig. 3.** FT-IR spectra of $NH_2$-MIL-101(Fe) and MIL-101(Fe).

spectral differences between $NH_2$-MIL-101(Fe) and MIL-101(Fe). Peaks at 1256 $cm^{-1}$ and 3378 $cm^{-1}$ for the $NH_2$-MIL-101(Fe) spectrum correspond to the stretching vibrations of C—N and N—H in $NH_2$-BDC (Fig. 3). These results confirm the presence of amine groups on the $NH_2$-MIL-101(Fe) surface. Furthermore, the FT-IR spectra revealed strong bands at 1392 and 1591 $cm^{-1}$, which were attributed to the asymmetric (as(C═O)) and symmetric (s(C═O)) vibrations of carboxyl groups in BDC and $NH_2$-BDC, respectively [36]. The weak peaks at 1653 $cm^{-1}$ correspond to the υ(C═O) stretch of carboxyl groups in $H_2$BDC and $NH_2$-BDC [37], and the peak at 768 $cm^{-1}$ corresponds to the C—H vibration of the benzene ring [38]. Additionally, the peak at 3420 $cm^{-1}$ was assigned to the stretching vibration mode of the O—H bond. These FT-IR results document the existence of abundant functional groups on the MIL-101s surface.

Zeta potential was measured to determine surface charge characteristics of MIL-101s in aqueous solution as a function of pH. The points of zero charge (PZC) for MIL-101(Fe) and $NH_2$-MIL-101(Fe) were observed at pH 5.86 and 6.04, respectively (Fig. 4A). The similar PZC for the two MIL-101s suggests only slight differences due to amine groups on surface charge characteristics. The hydrophilicity of the MIL-101s was indirectly assessed by determining contact angles. Both MIL-101s displayed strong hydrophilicity (Fig. S2) signifying a strong affinity for hydrophilic target analytes and weak hydrophobic interactions with non-polar compounds.

### 3.2. Comparison of extraction performances by MIL-101s

The DSPE of 10 BPs and their derivatives by MIL-101s was carried out at a fortification level of 20.0 μg $L^{-1}$. The extraction recoveries (ERs) of BPs by MIL-101(Fe) increased gradually with increases in log $K_{ow}$ values (2.0–4.0) until reaching a maximum level for BPB having a log $K_{ow}$ value of 3.96 (Fig. 5). With further increases in log $K_{ow}$ from 4.53 (BPZ) to 6.12 (BPP), a decreasing trend for ERs was observed. Due to the strong hydrophilicity of MIL-101s and its weak hydrophobic interaction with nonpolar molecules, the extraction efficiency decreased as the log $K_{ow}$ increased in the range of 4.0–6.0 [39,40]. As the polarity of the analytes increased, the aqueous solution competed with the MOF for the target molecule. The higher the polarity of BPs and their derivatives (log $K_{ow}$ = 2.0–4.0), the stronger their hydrophilicity, which resulted in decreased adsorption of analytes by the MOF and therefore decreased ERs. It is noteworthy that the ERs for BPF (log $K_{ow}$ = 2.73) and BPE (log $K_{ow}$ = 3.08) were ~39.2% and 81.8% by MIL-101(Fe), but were increased to 76.4% and 92.3% with $NH_2$-MIL-101(Fe), respectively. This was not the case for weakly polar BPs (log $K_{ow}$ ≥ 3.43) containing —OH groups, including BPA, BPB, BPZ, BPAP and BPP. As for bisphenol derivatives, $NH_2$-MIL-101(Fe) gave a 1.63-fold higher ER for BFDGE·$2H_2O$ (log $K_{ow}$ = 1.07) than MIL-101(Fe), and a comparable ER for BADGE·$2H_2O$ (log $K_{ow}$ = 1.86). In contrast, $NH_2$-MIL-101(Fe) gave only a 35.4% ER for weakly polar BADGE (log $K_{ow}$ = 3.95), which was much lower than that of MIL-101(Fe) (56.0%). These results demonstrate that ΔERs > 0 or ≈0 (ΔERs = ER $NH_2$-MIL-101(Fe) − ER MIL-101(Fe)) were observed for BPs containing —OH groups, and ΔERs values decreased with an increase in log $K_{ow}$. In contrast, ΔERs < 0 were observed for BADGE compounds not containing —OH groups suggesting that the amino-functionalized MOF was not effective in enhancing the extraction efficiency of BADGE. Mechanistically, this indicates interaction between the amino group and —OH groups on BPs; therefore BPs not containing —OH groups lacked strong interactions with $NH_2$-MIL-101(Fe). Additionally, the $S_{BET}$ of $NH_2$-MIL-101(Fe) was smaller than that of MIL-101(Fe).

For MIL-101(Fe), BPs with highly delocalized π electrons allow π-π interaction with the terephthalic acid molecules in the framework, and π-complexation between the π-electrons of aromatic rings and Lewis acidic sites ($Fe^{3+}$ centers) in the pores of MIL-101(Fe). Although the amino-functionalized material had similar structures and properties as MIL-101(Fe), they demonstrated an obvious difference in ERs for different BPs. The surface properties including zeta potential and contact angle were basically the same, while the $S_{BET}$ and pore size of MIL-101(Fe) was slightly larger than $NH_2$-MIL-101(Fe) (Table 2), which

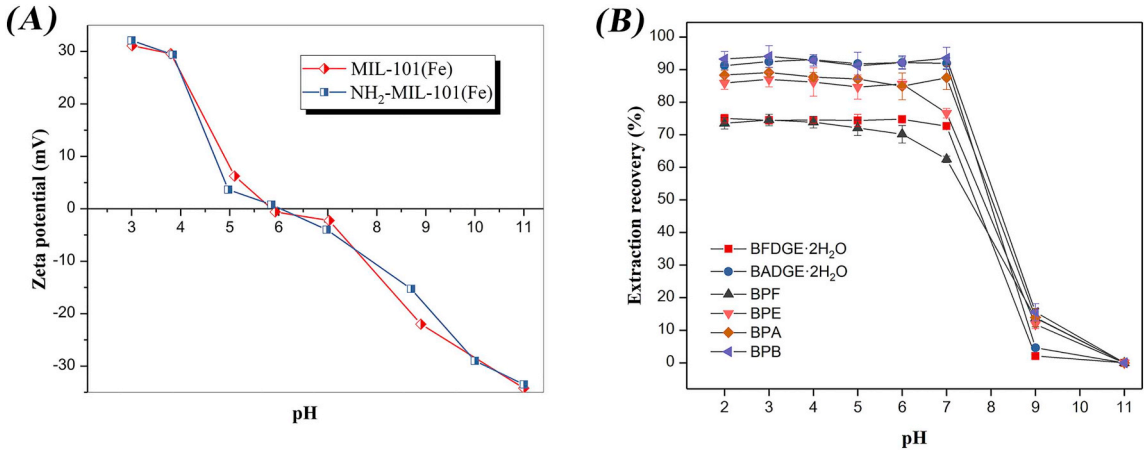


**Fig. 4.** Zeta potential of MIL-101s as a function of pH (A, lines do not necessarily represent linear trends), and effect of the pH on extraction efficiency of BPs (B, fortification level of 20 μg $L^{-1}$).

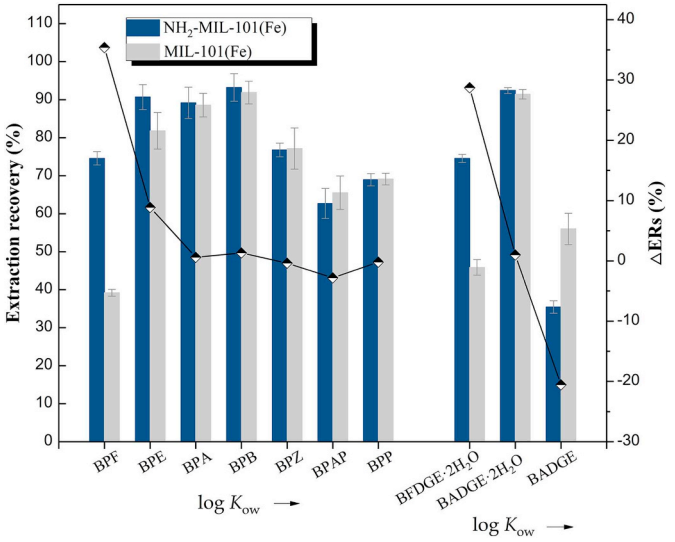


**Fig. 5.** Comparison of extraction recovery of 10 BPs between $NH_2$-MIL-101(Fe) and MIL-101(Fe).

**Table 2**
Surface properties of MIL-101s.

| MIL-101 MOF | $S_{BET}$ ($m^2 \cdot g^{-1}$) | $V_{Avg.}$ ($m^3 \cdot g^{-1}$) | $W_{Avg.}$ (nm) | ZPC | $\theta_c$ |
|---|---|---|---|---|---|
| $NH_2$-MIL-101(Fe) | 2914 | 1.46 | 2.19 | pH = 6.04 | 0° |
| MIL-101(Fe) | 3067 | 1.79 | 2.24 | pH = 5.86 | 0° |

Note: ZPC: zero point of charge; $\theta_c$: contact angle.

should be conducive to the extraction of BPs by $NH_2$-MIL-101(Fe). Therefore, hydrogen-bonding is assumed to play an important role in determining the ERs for BPs because the N-H group is a putative basic site contributing to formation of hydrogen bonds. Although the amino group in $NH_2$-MIL-101(Fe) only provides a weak Brønsted basic site, it presumably provides acid-base interactions with BPs, which are weakly acidic compounds with p*K*a values of 9.91–15.32 (Table 1). This also indicates that acid − base interactions were not a key factor influencing adsorption capacity. In addition, many reports have reported that materials can achieve better results in solid phase extraction through amino modification [41]. Therefore, the strong adsorption affinity is attributed to specific interactions between $NH_2$-MIL-101(Fe) and BPs. In order to verify this inference and determine the binding modes of BPs and their derivatives with MIL-101s, IR spectroscopy was applied to examine differences in BP interactions with $NH_2$-MIL-101(Fe) and MIL-101(Fe). IR spectroscopy is very suitable for detecting amino group interactions since the $\nu$(N−H) vibration is quite intense and strongly affected by formation of hydrogen donor-acceptor complexes. IR spectroscopy also provides a means to assess MOF stability after treatment with different BPs [42,43], and the treatment process was similar to the extraction method.

The IR spectrum resulting from treatment of 6 BPs containing O-H groups with $NH_2$-MIL-101(Fe) displays a band at 3378 $cm^{-1}$ indicating that the BP adsorption occurs through hydrogen bonds (Fig. 6A). This band was virtually absent in the untreated $NH_2$-MIL-101(Fe), since there was only a small amount of carboxyl groups on the MOF surface to form hydrogen bonds with the amino groups. In the case of $NH_2$-MIL-101(Fe), Fig. 6A illustrates strongly increased peak intensity after treatment with 0.05 to 5.0 mg $L^{-1}$ BPs containing O-H group. Further, a similar $\nu$(NH) band was present at the same wavenumber before and after treatment with BADGE without O-H groups (Fig. 6B), suggesting a lack of hydrogen bonding due to the absence of hydroxyl groups. In the case of MIL-101(Fe), no new bands were detected in the 3600–3200 $cm^{-1}$ region, suggesting that formation of hydrogen bonds was due to the presence of amino groups (Fig. 6C and D). Hence, the significant difference in adsorption efficiency for relatively polar BPs (BPF, BPE and BFDGE·$2H_2O$ with log $K_{ow}$ of 1.0–3.0) between the two MOFs lies in their differential formation of hydrogen bonds between hydroxyl group of target molecules and the amino groups of the amino-functionalized materials. For nonpolar BADGE, which does not contain O-H groups, the different adsorption characteristics by the two MOFs are mainly caused by their different specific surface area and pore structure. In conclusion, hydrogen bonds are very effective for extraction of polar organic contaminants (i.e., those with lower log $K_{ow}$ values) from aqueous solutions, and $S_{BET}$ and pore structure play an important role in extraction of nonpolar organic compounds in the absence of hydrogen bonding. Based on these results, we infer that hydrogen-bonding interactions are highly important for extraction of comparatively inert molecules, which usually are not easily extracted by other chemical means (e.g. acid-base interaction, π-π interaction, coordination etc.).

### 3.3. Optimization of extraction conditions

To extend the potential environmental application of $NH_2$-MIL-101(Fe) as an extraction adsorbent, we evaluated its use for the determination of BPs and their derivatives in real-world waters. A series of operational parameters affecting the ERs for BPs were assessed, including extraction adsorbent amount, extraction time, type and volume of elution solvent, elution time, and solution pH. To maximize extraction performance in terms of ERs, these operational factors were optimized through a series of experimental trials.

#### 3.3.1. Effect of sample pH

Solution pH has an important effect on ERs by affecting the molecular forms of target analytes, as well as the surface charge characteristics of the adsorbent [44]. For BPs and their derivatives, the pH of the aqueous media has a prominent impact on the dissociation of carboxyl and amine groups. The pH also influences ERs due to changes in hydrogen-bonding sites on both adsorbents and adsorbates (i.e., protonation and deprotonation) [45]. Similar mean ERs (80.78%–85.28%) were observed when pH values ranged from 2.0 to 7.0, but the ERs sharply decreased to zero when the pH was further increased from 7.0 to 11.0 (Fig. 4B). This pattern results from $NH_2$-MIL-101(Fe) being stable under acidic and neutral conditions, but it is easily hydrolyzed under alkaline conditions resulting in collapse of the skeleton structure. The pH increase from 6.0 to 7.0 led to a slight decrease of ERs (ca. 2.1–9.0%) for relatively polar BPF and BPE by $NH_2$-MIL-101(Fe). To further understand this phenomenon, we analyzed the surface charge characteristics of amino-functionalized MIL-101(Fe) by zeta potential measurements and determined a PZC of 6.04 (Fig. 4A). Therefore, the $NH_2$-MIL-101(Fe) surface was positively charged at pH values below the PZC and the system was stable from pH 2.0 to 6.0. The surface became negatively charged with the increase in pH from 6.0 to 7.0, hindering hydrogen-bonding interactions. Moreover, the collapse of the MIL skeleton appeared when the pH exceeded 7.0. As a consequence, the optimum solution acidity for maximum ERs occurred in the pH range of 2.0–6.0.

#### 3.3.2. Effect of extractant dosage

To optimize extraction efficiency for target analytes, the dosage of $NH_2$-MIL-101(Fe) was evaluated in the range of 10 to 50 mg. A 30 mg dose of extractant achieved maximum ERs for BPs given the large specific surface area and high adsorption efficiency of $NH_2$-MIL-101(Fe) (Fig. 7A). As the extractant amount was increased from 10 to 30 mg, ERs gradually increased from a mean value of 70.8 to 82.9%, but ERs decreased to 61.5% with increasing extractant amounts from 30 to 50 mg. The reason for the decrease at higher extractant dosages may result from 400 μL of methanol not being sufficient to completely elute

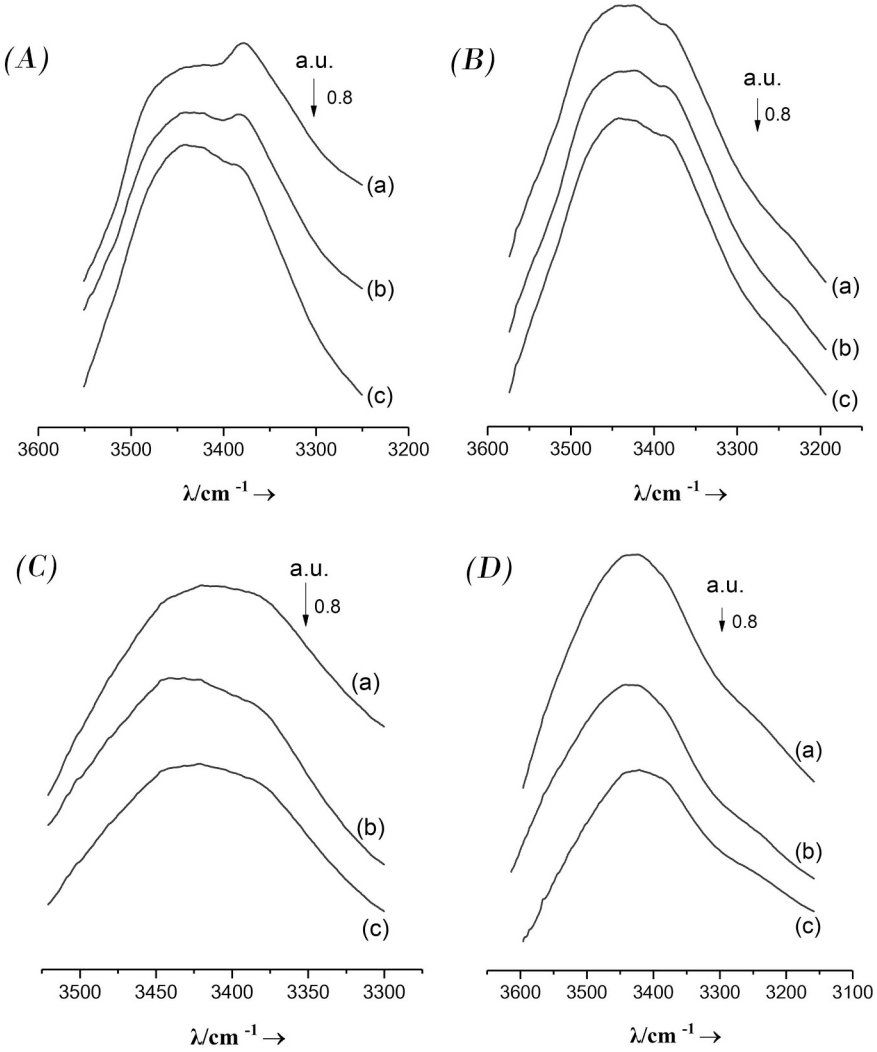


**Fig. 6.** Fundamental NH-stretching spectra of MIL-101 before (spectra a) and after treatment with 0.05 mg $L^{-1}$ BPs (spectra b) and 5 mg $L^{-1}$ BPs (spectra c): (A) spectra for $NH_2$-MIL-101(Fe) with 6 BPs, (B) for amino-MIL-101(Fe) with BADGE, (C) for MIL-101(Fe) with 6 BPs and (D) for MIL-101(Fe) with BADGE.

the target analytes from the excess extractant. Thus, 30 mg was selected as the optimal extractant dosage for the pretreatment procedure.

### 3.3.3. Effect of extraction time

The effect of extraction time on ERs was evaluated at times ranging from 1.0 to 5.0 min for the DSPE procedure. The ERs for BPs reached a maximum at 2.0 min, followed by a gradual decrease with a further increase in time from 2 to 5 min (Fig. 7B). The drop-off in ERs at longer extraction times may result from the longer ultrasonic treatment at strong energy levels leading to weaker hydrogen-bonding interaction and/or collapse of the MIL framework. Based on these results, the optimized extraction time was set at 2.0 min for subsequent experiments.

### 3.3.4. Selection of elution solvent type and volume

Elution solvent is required to recover the adsorbed target analytes from the adsorbent. Herein, four elution solvents were examined: methanol, acetonitrile, acetone and DMF. As shown in Fig. 7C, DMF gave the lowest mean ERs (~44.1%) except for BADGE·$2H_2O$, while methanol, acetonitrile and acetone yielded higher ERs (62.0–92.4%) following the order: methanol > acetone > acetonitrile. In addition, the volume of elution solvent must be sufficient to completely elute the analytes from the adsorbent while at the same time not being too large to avoid unduly diluting the sample. Therefore, the effects of methanol volume on ERs for BPs were investigated over the range of 200–800 μL. An elution solvent volume of 400 μL provided the highest ERs in the range of 73.1 to 92.4% (Fig. 7D). In comparison, when the volume was < 400 μL, the analytes were not totally eluted. Although the ERs remained nearly constant with increasing solvent volumes between 400 and 800 μL, the analyte concentrations and enrichment factor prominently decreased due to dilution. Therefore, a 400 μL methanol volume was employed as the optimum elution solvent and volume.

### 3.3.5. Effect of vortex elution time

An appropriate vortex time is necessary to effectively elude BPs adsorbed on $NH_2$-MIL-101(Fe). The vortex time was evaluated in the range of 1.0–5.0 min. There was no remarkable change in ERs for BPs when increasing the vortex time from 1.0 to 5.0 min (Fig. S3). As a result, a vortex time of 1.0 min was selected as the optimum level to speed operational throughput.

## 3.4. Analytical performance of $NH_2$-MIL-101(Fe)-based DSPE method

The optimized method was applied to detection of BPs and their derivatives in water samples. Linear ranges (LRs) spanned 0.05–0.44–200 μg $L^{-1}$ for BPs and their derivatives (Table 3) with coefficients of determination ($R^2$) ranging between 0.9986 and 0.9997.

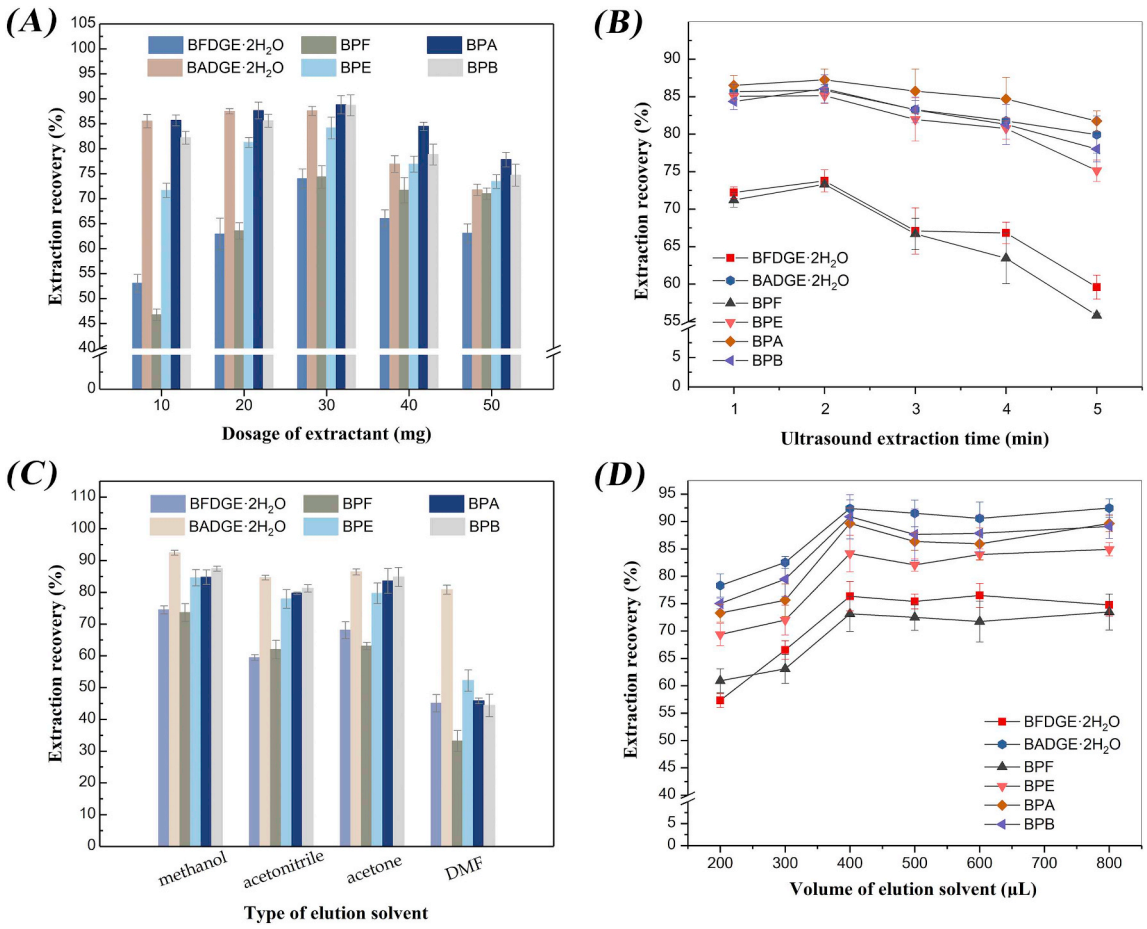


**Fig. 7.** Factors affecting the extraction efficiency for 20 μg $L^{-1}$ BPs, $NH_2$-MIL-101(Fe) dosage (A); extraction time (B); eluent type (C); and eluent volume (D). Error bars show the standard deviations for three replicate extractions.

**Table 3**
Analytical performance of the newly developed method.

| Analytes | Correlation coefficient ($R^2$) | Linear range (μg $L^{-1}$) | LOD (μg $L^{-1}$) | LOQ (μg $L^{-1}$) | Intra-day precision (RSD%, n = 6) | | | Inter-day precision (RSD%, n = 6) | | |
|---|---|---|---|---|---|---|---|---|---|---|
| | | | | | Low | Medium | High | Low | Medium | High |
| BFDGE·2$H_2O$ | 0.9997 | 0.08–200 | 0.024 | 0.08 | 0.9 | 3.6 | 3.3 | 7.6 | 2.6 | 4.3 |
| BADGE·2$H_2O$ | 0.9986 | 0.05–200 | 0.016 | 0.05 | 4.9 | 2.2 | 2.2 | 7.4 | 2.2 | 4.2 |
| BPF | 0.9997 | 0.17–200 | 0.050 | 0.17 | 2.0 | 3.3 | 1.8 | 6.6 | 1.6 | 4.2 |
| BPE | 0.9994 | 0.28–200 | 0.084 | 0.28 | 2.0 | 2.9 | 1.5 | 4.1 | 1.6 | 1.9 |
| BPA | 0.9997 | 0.34–200 | 0.101 | 0.34 | 2.3 | 3.7 | 1.2 | 5.5 | 1.9 | 2.8 |
| BPB | 0.9991 | 0.44–200 | 0.131 | 0.44 | 4.8 | 3.2 | 2.0 | 4.8 | 2.0 | 1.3 |

Note: LOD and LOQ denote limit of detection (S/N = 3) and limit of quantitation (S/N = 10), respectively. Treatments "high" "medium" and "low" indicate fortification concentrations of 50, 20 and 5 μg $L^{-1}$, respectively.

Limits of detection (LODs; S/N = 3) for BPs and their derivatives ranged from 0.016 to 0.131 μg $L^{-1}$, while limits of quantitation (LOQs; S/N = 10) were between 0.05 and 0.44 μg $L^{-1}$. At three spiked levels (5, 20 and 50 μg $L^{-1}$), the intra-day and inter-day precisions, expressed as relative standard deviations (RSDs) from six replicate determinations (n = 6), were in the range of 0.9–4.9% and 1.3–7.6%, respectively (Table 3). To evaluate the applicability of the $NH_2$-MIL-101(Fe)-based DSPE method for real-world samples, three different waters (sea, river and tap waters) were tested for the quantification of trace-levels of BPs and their derivatives. Because the pH values of three water samples after adding $NH_2$-MIL-101(Fe) were 5.58, 4.03 and 3.15, respectively, we did not adjust the solution pH. The optimized method gave relative recoveries of 90.8–117.8% for spiked samples, indicating that the newly developed method could meet requirements for trace-level analysis of BPs and their derivatives in environmental waters (Table 4). Concentrations of BADGE·2$H_2O$ and BPF in non-spiked samples were 4.33 ± 0.93 μg $L^{-1}$ and 0.24 ± 0.05 μg $L^{-1}$ in the river water, respectively (Table 4), which were similar to concentrations previously

**Table 4**
Analytical results for BPs and their derivatives in environmental water samples (mean ± SD, n = 3).

| Analytes | Sea water | | | | River water | | | | Tap water | | | |
|---|---|---|---|---|---|---|---|---|---|---|---|---|
| | Non-spiked | Spiked ($\mu g\,L^{-1}$) | Detected ($\mu g\,L^{-1}$) | RR (%) | Non-spiked | Spiked ($\mu g\,L^{-1}$) | Detected ($\mu g\,L^{-1}$) | RR (%) | Non-spiked | Spiked ($\mu g\,L^{-1}$) | Detected ($\mu g\,L^{-1}$) | RR (%) |
| BFDGE·2H$_2$O | ND | 5 | 5.15 ± 0.03 | 103.0 | ND | 5 | 5.10 ± 0.06 | 102.0 | ND | 5 | 5.29 ± 0.14 | 105.8 |
| | | 20 | 22.21 ± 0.31 | 111.1 | | 20 | 19.17 ± 0.29 | 95.8 | | 20 | 20.40 ± 0.46 | 102.0 |
| | | 50 | 47.38 ± 0.52 | 94.8 | | 50 | 48.39 ± 0.65 | 96.8 | | 50 | 50.80 ± 0.85 | 101.6 |
| BADGE·2H$_2$O | ND | 5 | 5.89 ± 0.30 | 117.8 | 4.33 ± 0.93 | 5 | 9.95 ± 0.16 | 112.3 | ND | 5 | 5.63 ± 0.05 | 112.6 |
| | | 20 | 20.13 ± 0.20 | 100.7 | | 20 | 22.67 ± 0.19 | 91.7 | | 20 | 21.64 ± 0.46 | 108.2 |
| | | 50 | 45.39 ± 0.91 | 90.8 | | 50 | 52.66 ± 2.62 | 96.66 | | 50 | 48.80 ± 1.54 | 97.6 |
| BPF | ND | 5 | 5.10 ± 0.13 | 102.1 | 0.24 ± 0.05 | 5 | 5.32 ± 0.13 | 101.7 | ND | 5 | 5.75 ± 0.13 | 115.0 |
| | | 20 | 22.32 ± 0.35 | 111.6 | | 20 | 20.63 ± 0.92 | 101.9 | | 20 | 21.86 ± 0.40 | 109.3 |
| | | 50 | 50.88 ± 0.55 | 101.8 | | 50 | 50.01 ± 0.37 | 99.5 | | 50 | 52.24 ± 0.93 | 104.5 |
| BPE | ND | 5 | 5.05 ± 0.07 | 101.1 | ND | 5 | 5.16 ± 0.26 | 103.2 | ND | 5 | 5.15 ± 0.18 | 103.1 |
| | | 20 | 20.47 ± 0.52 | 102.4 | | 20 | 20.48 ± 0.47 | 102.4 | | 20 | 20.79 ± 0.76 | 103.9 |
| | | 50 | 49.20 ± 0.64 | 98.4 | | 50 | 51.81 ± 1.91 | 103.6 | | 50 | 48.37 ± 0.96 | 96.7 |
| BPA | ND | 5 | 5.46 ± 0.15 | 109.2 | ND | 5 | 5.00 ± 0.06 | 100.0 | ND | 5 | 5.29 ± 0.20 | 105.8 |
| | | 20 | 20.52 ± 0.42 | 102.6 | | 20 | 19.66 ± 0.45 | 98.3 | | 20 | 20.52 ± 0.56 | 102.6 |
| | | 50 | 46.57 ± 0.42 | 93.1 | | 50 | 50.05 ± 0.51 | 100.1 | | 50 | 49.49 ± 1.14 | 99.0 |
| BPB | ND | 5 | 5.43 ± 0.22 | 108.5 | ND | 5 | 5.56 ± 0.05 | 111.2 | ND | 5 | 4.85 ± 0.12 | 97.4 |
| | | 20 | 21.25 ± 0.28 | 106.2 | | 20 | 17.93 ± 0.08 | 89.7 | | 20 | 18.79 ± 0.22 | 94.0 |
| | | 50 | 46.83 ± 0.40 | 93.7 | | 50 | 46.67 ± 0.41 | 93.3 | | 50 | 48.07 ± 1.04 | 96.1 |

Note: (1) RR indicates the relative recovery; (2) SD indicates standard deviation; and (3) ND denotes non-detectable.

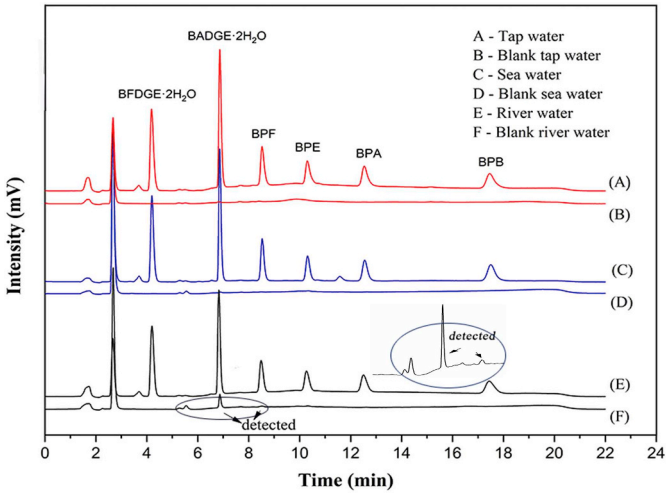


**Fig. 8.** Typical chromatograms of the BPs in environmental waters before and after spiking.

reported in the literature [8,9,46]; all other analyte concentrations were below the LOD. A typical chromatogram for BPs in environmental water samples before and after spiking is shown in Fig. 8.

### *3.5. Comparison of the $NH_2$-MIL-101(Fe)-based DSPE method with other methods*

The analytical performance of the proposed $NH_2$-MIL-101(Fe)-based DSPE-HPLC-FLD method was compared with other commonly used methods for BP determination [47–52]. As generalized in Table 5, the $NH_2$-MIL-101(Fe)-based DSPE method showed low LODs, which were 2–9.9-fold lower than the MagG@PDA@Zr-MOF-DSPE-HPLC method [47], 15.3–44-fold lower than the MIPMS-SPE-HPLC method [48], and 7.6–22-fold lower than the DMIP-SPE-HPLC method [49]. These comparisons indicate that the newly developed method has superior sensitivity for determination of BPs at trace levels in environmental waters. Additional benefits of the new method include a rapid adsorption and elution process that can be achieved in 3 min, and very low organic solvent usage compared to other methods. Therefore, the Fe-based MOF was demonstrated to be an efficient adsorbent for simultaneous determination of BPs in real-world water samples. In sum, the proposed method based on $NH_2$-MIL-101(Fe) exhibited comparable ERs, low LODs, low organic solvent consumption, simple pretreatment operations, and short analysis times compared to other methods.

## 4. Conclusions

We synthesized two structurally similar MIL-101s (virgin and amino-functionalized) as model sorbents, and analyzed their mechanistic interactions with BPs and their derivatives. The extraction efficiencies between $NH_2$-MIL-101(Fe) and MIL-101(Fe) were compared for extraction/preconcentration of 10 BPs in environmental waters. As for the relatively polar BPs (low log $K_{ow}$ values), hydrogen-bonding interaction played an important role in determining the extraction efficiency; however, $S_{BET}$ and pore structure were the key factors for extraction of BPs derivatives (lack of hydrogen bonding). By choosing appropriate pollutants and designing novel nanosorbents to form hydrogen-bonding interaction among molecules, the proposed method can also be applied to other extraction systems. Additionally, the newly developed $NH_2$-MIL-101(Fe)-based DSPE method demonstrated good linearity, low LODs, and high reproducibility for the preconcentration and determination of trace-level BPs and their derivatives with contrasting polarities in complex environmental waters. The mechanistic analysis on H-bonding interaction between sorbent and contaminant lays theoretical foundation for designing novel nanosorbent materials. Moreover, the newly synthesized $NH_2$-MIL-101(Fe) sorbent has the great application potential in pretreatment of trace pollutants in real-world aqueous environments.

Supplementary data to this article can be found online at https://doi.org/10.1016/j.microc.2018.12.013.

**Table 5**
Comparison of the present work with other methods using different DSPE/SPE sorbents for the simultaneous determination of bisphenols and their derivatives.

| Extraction method | Adsorbent | Adsorption time (min) | Desorption time (min) | Volume of organic solvent (mL) | Matrix | LOD ($\mu g\ L^{-1}$/$\mu g\ kg^{-1}$) | Recovery (%) | RSD (%) | Ref. |
|---|---|---|---|---|---|---|---|---|---|
| DSPE-HPLC | MagG@PDA@Zr-MOF | 10 | 15 | – | Water | 0.1–1 | 67.9–92.9 | 0.62–4.89 | [47] |
| SPE-HPLC | MIPMS | – | – | 6.0 | Urine | 1.2–2.2 | 81.3–106.7 | 1.1–8.3 | [48] |
| SPE-HPLC | DMIP | – | – | 6.5 | Water | 0.6–1 | 82–102 | 0.2–4 | [49] |
| DMSPE- UPLC-MS/MS | PAX | 0.67 | – | 2.0 | Edible oils | 0.1–0.4 | 87.3–108 | < 11 | [50] |
| SPE-HPLC | HPCS | 0.5 | – | 4.0 | Water, soft drinks | 0.05–0.53 | 89.6–111.5 | 0.8–6.3 | [51] |
| MSPE-HPLC | 3DG/$ZnFe_2O_4$ | 15 | 2 | 1.96 | Water | 0.05–0.18 | 95.1–103.8 | < 6.2 | [52] |
| DSPE-HPLC | $NH_2$-MIL-101(Fe) | 2 | 1 | 0.4 | Water | 0.02–0.13 | 73.1–92.4 | 0.9–7.6 | This work |

Note: (1) MagG@PDA@Zr-MOF: magnetic graphene @ polydopamine @ Zr-MOF; (2) MIPMS: molecularly imprinted polymer microspheres; (3) DMIP: dummy molecularly imprinted polymers; (4) PAX: polymer anion exchange; (5) HPCS: hollow porous carbon sphere; (6) 3DG/$ZnFe_2O_4$: three dimensional graphene/$ZnFe_2O_4$.

## Acknowledgement

This work was jointly supported by the National Natural Science Foundation of China (21876125, 21707105 and 21577107), the Zhejiang Provincial Public Benefit Project (LGF18B070004), the Zhejiang Provincial Natural Science Foundation (LY19B070010), and the Suzhou Municipal Science and Technology Bureau Project (SYG201815).

## Conflict of interest

The authors declare that they have no competing interests.

## References

[1] E. Diamanti-Kandarakis, J.P. Bourguignon, L.C. Giudice, R. Hauser, G.S. Prins, A.M. Soto, R.T. Zoeller, A.C. Gore, Endocrine-disrupting chemicals: an endocrine society scientific statement, Endocr. Rev. 30 (2009) 293–342.
[2] J. Moreman, O. Lee, M. Trznadel, A. David, T. Kudoh, C.R. Tyler, Acute toxicity, teratogenic, and estrogenic effects of bisphenol A and its alternative replacements bisphenol S, bisphenol F, and bisphenol AF in zebrafish embryo-larvae, Environ. Sci. Technol. 51 (2017) 12796–12805.
[3] H. Wang, A. Zhang, W. Wang, M. Zhang, H. Liu, X. Wang, Separation and determination of triclosan and bisphenol A in water samples by dispersive liquid-iquid microextraction combined with capillary zone electrophoresis-UV detection, J. AOAC Inter. 96 (2013) 459–465.
[4] X. Zhao, L. Fu, J. Hu, J. Li, H. Wang, X. Wang, Analysis of PAHs in water and fruit juice samples by DLLME combined with LC-fluorescence detection, Chromatographia 69 (2009) 1385–1389.
[5] X. Sun, J. Wang, Y. Li, J. Jin, B. Zhang, S.M. Shah, X. Wang, J. Chen, Highly selective dummy molecularly imprinted polymer as a solid-phase extraction sorbent for five bisphenols in tap and river water, J. Chromatogr. A 1343 (2014) 33–41.
[6] W.T. Tsai, Human health risk on environmental exposure to bisphenol-A: a review, J. Environ. Sci. Health C Environ. Carcinog. Ecotoxicol. Rev. 24 (2006) 225–255.
[7] L.N. Vandenberg, I. Chahoud, J.J. Heindel, V. Padmanabhan, F.J. Paumgartten, G. Schoenfelder, Urinary, circulating, and tissue biomonitoring studies indicate widespread exposure to bisphenol A, Environ. Health Perspect. 118 (2010) 1055–1070.
[8] D. Chen, K. Kannan, H. Tan, Z. Zheng, Y.L. Feng, Y. Wu, M. Widelka, Bisphenol analogues other than BPA: environmental occurrence, human exposure, and toxicity-a review, Environ. Sci. Technol. 50 (2016) 5438–5453.
[9] E. Yamazaki, N. Yamashita, S. Taniyasu, J. Lam, P.K. Lam, H.B. Moon, Y. Jeong, P. Kannan, H. Achyuthan, N. Munuswamy, K. Kannan, Bisphenol A and other bisphenol analogues including BPS and BPF in surface water samples from Japan, China, Korea and India, Ecotoxicol. Environ. Saf. 122 (2015) 565–572.
[10] C. Liao, K. Kannan, Concentrations and profiles of bisphenol A and other bisphenol analogues in foodstuffs from the United States and their implications for human exposure, J. Agric. Food Chem. 61 (2013) 4655–4662.
[11] C. Liao, F. Liu, Y. Guo, H.B. Moon, H. Nakata, Q. Wu, K. Kannan, Occurrence of eight bisphenol analogues in indoor dust from the United States and several Asian countries: implications for human exposure, Environ. Sci. Technol. 46 (2012) 9138–9145.
[12] O.M. Yaghi, M. O'Keeffe, N.W. Ockwig, H.K. Chae, M. Eddaoudi, J. Kim, Reticular synthesis and the design of new materials, Nature 423 (2003) 705–714.
[13] N.A. Khan, Z. Hasan, S.H. Jhung, Adsorptive removal of hazardous materials using metal-organic frameworks (MOFs): a review, J. Hazard. Mater. 244–245 (2013) 444–456.
[14] J.R. Li, R.J. Kuppler, H.C. Zhou, Selective gas adsorption and separation in metal-organic frameworks, Chem. Soc. Rev. 38 (2009) 1477–1504.
[15] C.I. Ezugwu, M.A. Asraf, X. Li, S. Liu, C.M. Kao, S. Zhuiykov, F. Verpoort, Selective and adsorptive removal of anionic dyes and $CO_2$ with azolium-based metal-organic frameworks, J. Colloid Interface Sci. 519 (2018) 214–223.
[16] G. Wu, J. Ma, S. Li, J. Guan, B. Jiang, L. Wang, J. Li, X. Wang, L. Chen, Magnetic copper-based metal organic framework as an effective and recyclable adsorbent for removal of two fluoroquinolone antibiotics from aqueous solutions, J. Colloid Interface Sci. 528 (2018) 360–371.
[17] K.M. Taylor-Pashow, J. Della Rocca, Z. Xie, S. Tran, W. Lin, Postsynthetic modifications of iron-carboxylate nanoscale metal-organic frameworks for imaging and drug delivery, J. Am. Chem. Soc. 131 (2009) 14261–14263.
[18] J. Della Rocca, D. Liu, W. Lin, Nanoscale metal-organic frameworks for biomedical imaging and drug delivery, Acc. Chem. Res. 44 (2011) 957–968.
[19] T. Uemura, N. Yanai, S. Kitagawa, Polymerization reactions in porous coordination polymers, Chem. Soc. Rev. 38 (2009) 1228–1236.
[20] M. Kurmoo, Magnetic metal-organic frameworks, Chem. Soc. Rev. 38 (2009) 1353–1379.
[21] J. Lee, O.K. Farha, J. Roberts, K.A. Scheidt, S.T. Nguyen, J.T. Hupp, Metal-organic framework materials as catalysts, Chem. Soc. Rev. 38 (2009) 1450–1459.
[22] J. Rocha, L.D. Carlos, F.A. Paz, D. Ananias, Luminescent multifunctional lanthanides-based metal-organic frameworks, Chem. Soc. Rev. 40 (2011) 926–940.
[23] V.G. Ponomareva, K.A. Kovalenko, A.P. Chupakhin, D.N. Dybtsev, E.S. Shutova, V.P. Fedin, Imparting high proton conductivity to a metal-organic framework

material by controlled acid impregnation, J. Am. Chem. Soc. 134 (2012) 15640–15643.
[24] S. Zhang, Z. Jiao, W. Yao, A simple solvothermal process for fabrication of a metal-organic framework with an iron oxide enclosure for the determination of organophosphorus pesticides in biological samples, J. Chromatogr. A 1371 (2014) 74–81.
[25] A. Oxana Kholdeeva, Y. Igor Skobelev, A. Konstantin Kovalenko, P. Vladimir Fedin, Solvent-free allylic oxidation of alkenes with O-2 mediated by Fe- and Cr-MIL-101, J. Catal. 298 (2013) 61–69.
[26] C. Qi, Q. Cai, P. Zhao, X. Jia, N. Lu, L. He, X. Hou, The metal-organic framework MIL-101(Cr) as efficient adsorbent in a vortex-assisted dispersive solid-phase extraction of imatinib mesylate in rat plasma coupled with ultra-performance liquid chromatography/mass spectrometry: application to a pharmacokinetic study, J. Chromatogr. A 1449 (2016) 30–38.
[27] S.H. Huo, X.P. Yan, Facile magnetization of metal-organic framework MIL-101 for magnetic solid-phase extraction of polycyclic aromatic hydrocarbons in environmental water samples, Analyst 137 (2012) 3445–3451.
[28] R. Dargahi, H. Ebrahimzadeh, Dispersive magnetic solid-phase extraction of phthalate esters from water samples and human plasma based on a nanosorbent composed of MIL-101(Cr) metal-organic framework and magnetite nanoparticles before their determination by GC–MS, J. Sep. Sci. 41 (2018) 948–957.
[29] Y. Hu, Z. Huang, J. Liao, G. Li, Chemical bonding approach for fabrication of hybrid magnetic metal-organic framework-5: high efficient adsorbents for magnetic enrichment of trace analytes, Anal. Chem. 85 (2013) 6885–6893.
[30] P. Rocio-Bautista, P. Gonzalez-Hernandez, V. Pino, J. Pasan, A.M. Afonso, Metal-organic frameworks as novel sorbents in dispersive-based microextraction approaches, Trends Anal. Chem. 90 (2017) 114–134.
[31] J.Y. Song, S.H. Jhung, Adsorption of pharmaceuticals and personal care products over metal-organic frameworks functionalized with hydroxyl groups: quantitative analyses of H-bonding in adsorption, Chem. Eng. J. 322 (2017) 366–374.
[32] X. Li, W. Guo, Z. Liu, R. Wang, H. Liu, Quinone-modified $NH_2$-MIL-101(Fe) composite as a redox mediator for improved degradation of bisphenol A, J. Hazard. Mater. 324 (2017) 665–672.
[33] O.I. Lebedev, F. Millange, C. Serre, G. Van Tendeloo, G. Férey, First direct imaging of giant pores of the metal–organic framework MIL-101, Chem. Mater. 17 (2005) 6525–6527.
[34] L. Chi, Q. Xu, X. Liang, J. Wang, X. Su, Iron-based metal-organic frameworks as catalysts for visible light-driven water oxidation, Small 12 (2016) 1351–1358.
[35] Z. Huang, S. Liu, J. Xu, L. Yin, J. Zheng, N. Zhou, G. Ouyang, Porous organic polymers with different pore structures for sensitive solid-phase microextraction of environmental organic pollutants, Anal. Chim. Acta 989 (2017) 21–28.
[36] X. Li, W. Guo, Z. Liu, R. Wang, H. Liu, Fe-based MOFs for efficient adsorption and degradation of acid orange 7 in aqueous solution via persulfate activation, Appl. Surf. Sci. 369 (2016) 130–136.
[37] H. Lu, H. Zhang, J. Wang, J. Zhou, Y. Zhou, A novel quinone/reduced graphene oxide composite as a solid-phase redox mediator for chemical and biological Acid Yellow 36 reduction, RSC Adv. 4 (2014) 47297–47303.
[38] B.C. Smith, Distinguishing structural isomers: mono- and disubstituted benzene rings, Spectroscopy 31 (2016) 36–39.
[39] A. Moral, M.D. Sicilia, S. Rubio, D. Perez-Bendito, Multifunctional sorbents for the extraction of pesticide multiresidues from natural waters, Anal. Chim. Acta 608 (2008) 61–72.
[40] Y. Li, Z. Yang, Y. Wang, Z. Bai, T. Zheng, X. Dai, S. Liu, D. Gui, W. Liu, M. Chen, L. Chen, J. Diwu, L. Zhu, R. Zhou, Z. Chai, T.E. Albrecht-Schmitt, S. Wang, A mesoporous cationic thorium-organic framework that rapidly traps anionic persistent organic pollutants, Nat. Commun. 8 (2017) 1354.
[41] H.R. Noormohamadi, M.R. Fat'hi, M. Ghaedi, Fabrication of polyethyleneimine modified cobalt ferrite as a new magnetic sorbent for the micro-solid phase extraction of tartrazine from food and water samples, J. Colloid Interface Sci. 531 (2018) 343–351.
[42] K.H. Moller, A.S. Hansen, H.G. Kjaergaard, Gas phase detection of the NH-P hydrogen bond and importance of secondary interactions, J. Phys. Chem. A 119 (2015) 10988–10998.
[43] B. Van de Voorde, M. Boulhout, F. Vermoortele, P. Horcajada, D. Cunha, J.S. Lee, J.-S. Chang, E. Gibson, M. Daturi, J.-C. Lavalley, A. Vimont, I. Beurroies, D.E. De Vos, N/S-heterocyclic contaminant removal from fuels by the mesoporous metal-organic framework MIL-100: the role of the metal ion, J. Am. Chem. Soc. 135 (2013) 9849–9856.
[44] N. Li, Q. Zhu, Y. Yang, J. Huang, X. Dang, H. Chen, A novel dispersive solid-phase extraction method using metal-organic framework MIL-101 as the adsorbent for the analysis of benzophenones in toner, Talanta 132 (2015) 713–718.
[45] J.Y. Song, I. Ahmed, P.W. Seo, S.H. Jhung, UiO-66-type metal–organic framework with free carboxylic acid: versatile adsorbents via H-bond for both aqueous and nonaqueous phases, ACS Appl. Mater. Interfaces 8 (2016) 27394–27402.
[46] Z. Yan, Y. Liu, K. Yan, S. Wu, Z. Han, R. Guo, M. Chen, Q. Yang, S. Zhang, J. Chen, Bisphenol analogues in surface water and sediment from the shallow Chinese freshwater lakes: occurrence, distribution, source apportionment, and ecological and human health risk, Chemosphere 184 (2017) 318–328.
[47] X. Wang, C. Deng, Preparation of magnetic graphene@polydopamine@Zr-MOF material for the extraction and analysis of bisphenols in water samples, Talanta 144 (2015) 1329–1335.
[48] J. Yang, Y. Li, J. Wang, X. Sun, R. Cao, H. Sun, C. Huang, J. Chen, Molecularly imprinted polymer microspheres prepared by pickering emulsion polymerization for selective solid-phase extraction of eight bisphenols from human urine samples, Anal. Chim. Acta 872 (2015) 35–45.
[49] X. Sun, J. Wang, Y. Li, J. Jin, J. Yang, F. Li, S.M. Shah, J. Chen, Highly class-selective solid-phase extraction of bisphenols in milk, sediment and human urine samples using well-designed dummy molecularly imprinted polymers, J. Chromatogr. A 1360 (2014) 9–16.
[50] Y. Xian, Y. Wu, H. Dong, X. Guo, B. Wang, L. Wang, Dispersive micro solid phase extraction (DMSPE) using polymer anion exchange (PAX) as the sorbent followed by UPLC-MS/MS for the rapid determination of four bisphenols in commercial edible oils, J. Chromatogr. A 1517 (2017) 35–43.
[51] Z. Zhang, J. Zhang, Y. Wang, Y. Tong, L. Zhang, Controlled synthesis of hollow porous carbon spheres for enrichment and simultaneous determination of nine bisphenols from real samples, Talanta 167 (2017) 428–435.
[52] L. Wang, Z. Zhang, J. Zhang, L. Zhang, Magnetic solid-phase extraction using nanoporous three dimensional graphene hybrid materials for high-capacity enrichment and simultaneous detection of nine bisphenol analogs from water sample, J. Chromatogr. A 1463 (2016) 1–10.